Quantum nanoelectromechanics with electrons, quasi-particles and Cooper pairs: effective bath descriptions and strong feedback effects

Aashish A Clerk[1] **and Steven Bennett**

Department of Physics, McGill University, Rutherford Physics Building, 3600 Rue University, Montréal, QC, H3A 2T8 Canada
E-mail: aashish.clerk@mcgill.ca

Abstract. Using a quantum-noise approach, we discuss the physics of both normal metal and superconducting single-electron transistors (SSETs) coupled to mechanical resonators. Particular attention is paid to the regime where transport occurs via incoherent Cooper-pair tunnelling (either via the Josephson quasi-particle (JQP) or double JQP (DJQP) process). We show that, surprisingly, the back-action of tunnelling Cooper pairs (or superconducting quasi-particles) can be used to significantly cool the oscillator. We also discuss the physical origin of negative-damping effects in this system and how they can lead to a regime of strong electromechanical feedback, where despite a weak SET–oscillator coupling, the motion of the oscillator strongly effects the tunnelling of the Cooper pairs. We show that in this regime, the oscillator is characterized by an *energy-dependent effective temperature*. Finally, we discuss the strong analogy between back-action effects of incoherent Cooper-pair tunnelling and ponderomotive effects in an optical cavity with a moveable mirror; in our case, tunnelling Cooper pairs play the role of the cavity photons.

[1] Author to whom any correspondence should be addressed.

Contents

1. Introduction

There has been considerable recent interest in studying the properties of mechanical oscillators coupled to quantum mesoscopic conductors. Such 'quantum' nanoelectromechanical systems (NEMS) are interesting because of their ability (in some cases) to perform quantum-limited position detection [1]–[4] and their potential to be used in quantum-controlled applications [5]. In addition, they represent a new and interesting problem in the area of quantum-dissipative systems, as the tunnelling electrons (or quasi-particles or Cooper pairs) in the conductor act as a non-equilibrium, non-Gaussian dissipative bath for the mechanical oscillator. Theoretically, attention has largely focused on two systems: a normal-metal single-electron transistor (SET) coupled to an oscillator [3], [6]–[12] and a tunnel junction (or quantum point contact) coupled to an oscillator [4, 5, 13, 14]; both systems have also been studied experimentally [1, 2, 15]. In these devices, it has been predicted that for weak couplings, the back-action of the conductor essentially mimics the effects of an equilibrium thermal bath, with an effective temperature which is roughly proportional to the drain–source voltage in the conductor.

In this paper, we turn to the properties of a quantum NEMS, which is considerably more complicated than either the normal-metal SET–oscillator system or the tunnel junction plus oscillator system. We consider a superconducting single electron transistor (SSET) coupled to a nanomechanical oscillator, focusing on regimes where transport in the SSET is via the incoherent tunnelling of Cooper pairs (both the Josephson quasi-particle process (JQP) and the double JQP (DJQP)) [16, 17]. Such processes are attractive from a measurement point of view, as they have a high gain at a relatively low source–drain voltage. We also discuss the regime where transport through the SSET is due to the sequential tunnelling of quasi-particles. Using a quantum-noise approach, we show that in each of these regimes, the SSET provides the oscillator with a highly non-trivial effective environment. In particular, the effective temperature of the SSET can be much lower than the drain–source voltage in the SSET, meaning that considerable cooling can be accomplished; this is in stark contrast to the normal-metal SET and tunnel junction systems, where it is difficult to achieve cooling. In addition, the resonant nature of Cooper-pair tunnelling leads to the possibility of unstable regimes characterized by negative dissipation; we discuss

the strong electromechanical feedback that arises in these regimes and characterize the resulting stationary state of the oscillator. This state is highly non-thermal and can be described using an energy-dependent effective temperature. Finally, we point out that by using incoherent Cooper-pair tunnelling, one can come extremely close to reaching the quantum limit on the displacement sensitivity; in contrast, this is not possible with a normal-metal SET. Note that an SSET plus oscillator system was also studied recently using an alternative technique by Blencowe *et al* [18].

The paper is organized as follows. In section 2, we will review the effective bath description of a weakly coupled NEMS, paying special attention to how back-action damping arises both quantum mechanically and classically. In section 3, we introduce the SET plus oscillator system and calculate the back-action in the sequential tunnelling regime; our results here are applicable to a number of different systems, including a normal SET, a Coulomb-blockaded quantum dot and an SSET. In section 4, we calculate the back-action properties of incoherent Cooper-pair tunnelling, and give a physical interpretation of negative-damping effects that arise here. We point out the strong analogy between the SSET system and an optical cavity with a moveable mirror, where forces arising from cavity photons can lead to cooling and instabilities [19]–[21]; in our system, tunnelling Cooper pairs play the role of the photons. Finally, in section 5, we present results for the strong feedback regime that occurs as a result of these negative-damping instabilities.

2. Effective bath description and the origin of back-action damping

At first glance, the theoretical problem presented by an NEMS seems formidable: we need to understand how the back-action of our quantum conductor effects the oscillator, given that the conductor is typically in a far-from-equilibrium state and typically does not have Gaussian-noise properties. Luckily, for many systems of interest, the coupling between the oscillator and the conductor is sufficiently weak that the current in the conductor responds linearly to the motion of the oscillator. As is discussed extensively in [22], the back-action effects of the conductor in this case can be directly related to the quantum-noise properties of the uncoupled conductor. We assume that the oscillator is coupled to the conductor via a term in the Hamiltonian which is linear in x

$$H_{int} = -A\hat{x} \cdot \hat{F}. \tag{1}$$

Here, A is a dimensionless coupling constant; it needs to be sufficiently weak such that the conductor only responds linearly to the motion of the oscillator. The operator $\hat{F}$ describes the quantity in the conductor which couples to the oscillator; for the SSET, we will see that $\hat{F}$ is simply proportional to the charge on the central island. For simplicity, we will choose the oscillator's origin so that $\langle \hat{F} \rangle = 0$. $\hat{F}$ plays the role of a fluctuating back-action force; its unsymmetrized quantum-noise spectrum at zero coupling to the oscillator,

$$S_F(\omega) = \int_{-\infty}^{\infty} dt \, e^{i\omega t} \langle \hat{F}(t)\hat{F}(0) \rangle, \tag{2}$$

will play a central role. Note that as the conductor in our NEMS acts as a position detector of the oscillator, we will often refer to it as 'the detector' in what follows.

Taking our oscillator to have mass m and natural frequency Ω, and assuming that it is also coupled to an equilibrium Ohmic bath, one finds from perturbation theory in A that its motion is described by a classical Langevin equation [22]

$$m\ddot{x}(t) = -m\Omega^2 x(t) - m\gamma_0\dot{x} + \delta f_0(t) + f_{avg}(t) + \delta f(t). \tag{3}$$

This classical Langevin equation involves two fluctuating forces, $\delta f_0(t)$ and $\delta f(t)$; it may be used to calculate the fluctuations in $x(t)$ in terms of the spectral densities of the δf_0 and δf fluctuations, as well as the oscillator's response to an external force. *The answers obtained for both these quantities from equation (3) are in exact correspondence to what is found from a perturbative quantum-mechanical calculation, performed to lowest non-vanishing order in A* [22].

Consider the right-hand side (RHS) of this Langevin equation. The second and third terms on the RHS describe the effects of the equilibrium bath on the oscillator: γ_0 is the damping rate induced by this bath and $\delta f_0(t)$ is the corresponding fluctuating force. The fluctuation–dissipation theorem demands that the spectral density of the δf_0 fluctuations obey

$$S_{\delta f_0}(\omega) = m\gamma_0 \hbar\omega \coth[\hbar\omega/(2k_B T_0)], \tag{4}$$

where T_0 is the bath temperature. γ_0 and T_0 have a simple interpretation: if the oscillator were not coupled to the conductor, its quality factor would be $Q_0 = \Omega/\gamma_0$ (the 'intrinsic' quality factor of the oscillator) and its temperature would simply be T_0.

The remaining terms on the RHS of equation (3) describe the back-action of the conductor. $\delta f(t)$ is the fluctuating part of the back-action force; its spectral density is determined directly by the symmetrized quantum noise in the operator $\hat{F}$:

$$S_{\delta f}(\omega) = \frac{A^2}{2}\left[S_F(\omega) + S_F(-\omega)\right], \tag{5}$$

In contrast, $f_{avg}(t)$ is the average value of the back-action force; it arises because the conductor (and hence $\langle\hat{F}\rangle$) changes in response to the motion of the oscillator. We can write this force as the sum of a conservative force, which is in-phase with the oscillator's motion, and a damping force which is out-of-phase with the oscillator's motion

$$f_{avg}(t) = f_{damp}(t) + f_{cons}(t), \tag{6a}$$

$$f_{damp}(t) = -m\int_{-\infty}^{\infty} dt' \, \gamma(t-t')\dot{x}(t'), \tag{6b}$$

$$f_{cons}(t) = \int_{-\infty}^{\infty} dt' \, \alpha(t-t')x(t'). \tag{6c}$$

Using standard quantum linear response relations, one has

$$\lambda_F(t) = -\frac{i}{\hbar}\theta(t)\langle[F(t), F(0)]\rangle, \tag{7a}$$

$$m\gamma(\omega) = A^2\left(\frac{-\text{Im}\lambda_F(\omega)}{\omega}\right) = \frac{A^2}{\hbar}\left(\frac{S_F(\omega) - S_F(-\omega)}{2\omega}\right), \tag{7b}$$

$$\alpha(\omega) = A^2\left[-\text{Re}\lambda_F(\omega)\right]. \tag{7c}$$

Note that this description of the oscillator only requires A to be small enough that linear response is valid; there is no restriction on the size of the oscillator frequency Ω. Note also that the fluctuating back-action force $\delta f(t)$ will not in general be related to the damping kernel $\gamma(\omega)$ by a fluctuation–dissipation relation, as our conductor is generally not in an equilibrium state. Nonetheless, we may use the fluctuation–dissipation relation to *define* an effective temperature $T_{eff}(\omega)$ at each frequency ω via

$$\coth\left(\frac{\hbar\omega}{2k_B T_{eff}(\omega)}\right) \equiv \frac{S_{\delta f}(\omega)}{m\gamma\hbar\omega}. \tag{8}$$

In the most general case, the oscillator responds to a variety of frequencies, and thus we cannot characterize the back-action by a single temperature; in this case, the oscillator will not be in a thermal state. However, if the oscillator has a sufficiently high quality factor, it only responds to forces in a narrow frequency band centred on $\omega = \Omega$. If this frequency band is small enough, $T_{eff}(\omega)$ will be constant over its width. In this case, the back-action will appear to the oscillator as being due to an equilibrium bath having a temperature $T = T_{eff}(\Omega)$ and a damping rate $\gamma(\Omega)$. The spring constant $k = m\Omega^2$ of the oscillator will also be modified by the conservative part of the average back-action force; this will be given by

$$\Delta k = -\alpha(\Omega) = A^2[\text{Re}\lambda_F(\Omega)]. \tag{9}$$

Including the effects of the equilibrium bath coupled to the oscillator, equation (3) tells us that the oscillator will be in a thermal state, characterized by a total damping rate $\gamma(\Omega) + \gamma_0$ and a temperature T_{osc} given rigorously by [22]

$$T_{osc} = \frac{\gamma_0 T_0 + \gamma(\Omega)T_{eff}}{\gamma_0 + \gamma(\Omega)}. \tag{10}$$

We again stress that the effective bath description presented above can hold even if the oscillator frequency Ω is not small compared to the frequency scales of the conductor; all that is needed is that the 'mechanical bandwidth' of the oscillator should be small. Nonetheless, we are often interested in the case where $1/\Omega$ is long compared to the timescales relevant to the conductor; in this case, we can approximate $\gamma(\omega) \simeq \gamma(0)$, $\alpha(\omega) \simeq \alpha(0)$ and $S_{\delta f}(\omega) \simeq S_{\delta f}(0)$. This corresponds to a damping force $F_{damp} = -m\gamma(\omega = 0)\dot{x}$, a modified spring constant $\Delta k = -\alpha(\omega = 0)$ and a fluctuating back-action force with a white noise spectrum. In this case,

Institute *of* **Physics**   Φ DEUTSCHE PHYSIKALISCHE GESELLSCHAFT

equation (8) reduces to

$$k_B T_{eff} \equiv \frac{S_F(0)}{2\partial_\omega S_F(0)/\hbar} = \frac{A^2 S_F(0)}{2m\gamma}. \tag{11}$$

Before applying these ideas to the SET plus oscillator system, we comment on the origin of back-action damping, as there seems to have been some confusion on this point in the NEMS literature. Equation (7b) makes it clear that there are two equivalent ways of thinking about damping. The first equality tells us that damping is simply the out-of-phase response of the average value of the back-action force F to the position of the oscillator. The second equality gives us a quantum picture for damping: damping results from the absorption of energy from the oscillator by the 'bath' producing the force F (recall that positive-frequency noise corresponds to absorption of energy, while negative-frequency noise corresponds to emission of energy [23]).

There is another simple but useful classical way to understand both the origin of back-action damping and the spring-constant renormalization [19]–[21]. We simply need to use the fact that (i) the average back-action force $f_{avg}(t)$ is proportional to x, and (ii) the back-action force does not respond instantaneously to changes in the oscillator's motion. In the simple case, where the oscillator is much slower than the source of the back-action, we can take the time delay to be given exactly by τ_{resp}.[2] We thus have

$$f_{avg}(t) = f_{avg}[x(t - \tau_{resp})] \simeq \frac{\mathrm{d}f_{avg}}{\mathrm{d}x} \cdot x(t - \tau_{resp}) \simeq \frac{\mathrm{d}f_{avg}}{\mathrm{d}x} \cdot [x(t) - \tau_{resp}\dot{x}(t)]. \tag{12}$$

This immediately yields

$$\Delta k = -\frac{\mathrm{d}f_{avg}}{\mathrm{d}x}, \tag{13a}$$

$$m\gamma = \frac{\mathrm{d}f_{avg}}{\mathrm{d}x}\tau_{resp}. \tag{13b}$$

Thus, we can view the time delay in the response of the back-action force as being the origin of damping. Note that this argument tells us that Δk and γ should always have the opposite sign, and that their ratio gives us a measure of τ_{resp}, the response time of the conductor's back-action

$$\tau_{resp} \equiv -\frac{m\gamma}{\Delta k}. \tag{14}$$

As we will see, the concept of a back-action response time will be useful in understanding the back-action properties of various different mesoscopic systems.

---

[2] A more exact equation would be to say $f_{avg}(t) = \frac{\mathrm{d}f_{avg}}{\mathrm{d}x}\int_{-\infty}^{t}\mathrm{d}t'\exp[-(t-t')/\tau_{resp}]x(t')$. For $\Omega\tau_{resp} \ll 1$, this reduces to equation (12) above.

3. Back-action of electron and quasi-particle sequential tunnelling

An SET consists of a metallic island with a large Coulomb-charging energy $E_C = e^2/(2C_\Sigma)$ (C_Σ is the total capacitance of the island) coupled via tunnel junctions to both a source and a drain metal electrode; in the case of an SSET, the island and both the electrodes are super-conducting. The charging-energy term in the Hamiltonian is given by

$$H_C = E_C(\hat{n} - \mathcal{N})^2, \tag{15}$$

where $\hat{n}$ is the charge on the SET island and $\mathcal{N} = C_g V_g/e$ is the dimensionless electron number associated with a gate voltage V_g which is coupled to the island via a capacitance C_g. In addition, a voltage V_{SD} is applied between source and drain which drives the tunnelling of electrons across the SET.

To make an NEMS device involving an SET, a mechanical oscillator (coated with metal) is placed in proximity to the island of the SET such that there is a capacitive coupling C_{osc} between the charge on the SET island and the potential of the oscillator; C_{osc} depends on the island–oscillator distance. The oscillator is then voltage biased, with the result that changes in its displacement modify the electrostatic potential of the SET island (i.e. the parameter $\mathcal{N}$ becomes x dependent). For small displacements x, the result is a linear-in-x coupling term in the Hamiltonian[3]:

$$H_{int} = -A\hat{n}x, \tag{16}$$

where A is the effective coupling strength

$$A = 2E_C \frac{d\mathcal{N}}{dx} = 2E_C \left(\frac{V_{osc}}{e}\right) \frac{dC_{osc}}{dx} \simeq 2E_C \left(\frac{C_{osc}V_{osc}}{e}\right) \frac{1}{d} = eV_{osc} \left(\frac{C_{osc}}{C_\Sigma}\right) \frac{1}{d}. \tag{17}$$

Here, V_{osc} is the voltage applied to the oscillator and d is the oscillator–island spacing when the oscillator is in its equilibrium position; for more details, see, e.g. [10]. Comparing against equation (1), we see that $A\hat{n}$ plays the role of a fluctuating back-action force on the oscillator, and that it is the quantum-noise spectrum of the charge $\hat{n}$ that will determine the nature of this back-action. This conclusion is true regardless of where the SET is operated, or whether it is superconducting or normal.

Calculating the back-action thus reduces to a problem of calculating the quantum-noise spectrum of charge fluctuations in the SET. For various operating points of a SET/SSET, this has been done [23]–[28]. The simplest operating regime of an SET is that of sequential tunnelling. Current flow is due to electrons (or, in the case of an SSET, quasi-particles) incoherently tunnelling on and off the SET island via real, energy-conserving transitions; because of the large charging energy E_C, only two charge states of the island are involved in transport. The quantum charge noise in this regime was calculated in [23] by using a qubit as a theoretical quantum-noise spectrometer. In this approach, one first models the dynamics of a two-level system (TLS) weakly coupled to the SET island charge, and calculates an equation of motion for

---

[3] Note there is an additional term in the SET plus oscillator Hamiltonian, which is proportional to $V_{osc}^2 x^2$, and thus contributes a V_{osc}-dependent shift in the oscillator's frequency. This term has nothing to do with back-action: it is independent of the SET island charge $\hat{n}$. As such, we do not discuss it in what follows.

Institute *of* **Physics** Φ DEUTSCHE PHYSIKALISCHE GESELLSCHAFT

a reduced density-matrix tracking both the TLS state and the SET island charge; for sequential tunnelling, this is done to the lowest non-vanishing order in the tunnelling of an SET. In the limit of weak SET–TLS coupling, one can calculate both the stationary state of the TLS, as well as its relaxation rate. These may then be used to directly extract the finite frequency quantum-noise spectrum of $\hat{n}$ at the splitting frequency of the TLS. By varying this splitting frequency, one can extract the entire quantum-noise spectrum of $\hat{n}$.

Using the above approach, one finds that the low-frequency SET charge noise in the sequential tunnelling regime is simply telegraph noise, while the frequency-asymmetry in the noise is determined by how the tunnelling rates depend on energy [26, 28]. To be definite, consider a sequential-tunnelling process involving the island charge states $n = 0$ and 1, and consider the zero temperature limit. There are then two rates of interest: Γ_+, the rate at which electrons (or quasi-particles) hop onto the island from the left junction, and Γ_-, the rate at which electrons hop off the island through the right junction. The average current is given by $I = e\Gamma_+\Gamma_-/\Gamma_\Sigma$ (where $\Gamma_\Sigma = \Gamma_+ + \Gamma_-$), and the average island is $\langle n \rangle = e\Gamma_+/\Gamma_\Sigma$. It will also be important to know how these rates change if we either increase or reduce the amount of energy driving the given tunnel event; let E represent this additional added energy. Using equations (7b) and (11) and the results of [23], one obtains the following simple expressions for the back-action in the limit of small oscillator frequency (i.e. $\Omega \ll \Gamma_\Sigma$)

$$k_B T_{eff} = \frac{\Gamma_+\Gamma_-}{\partial_E (\Gamma_+\Gamma_-)}, \tag{18a}$$

$$m\gamma = A^2 \frac{\partial_E (\Gamma_+\Gamma_-)}{(\Gamma_\Sigma)^3}, \tag{18b}$$

$$\delta k = -(m\gamma) \times \Gamma_\Sigma. \tag{18c}$$

Here, each rate should be evaluated at $E = 0$. These expressions are equally valid for sequential tunnelling of electrons in an SET, electrons in a Coulomb-blockaded quantum dot or BCS quasi-particles in a SSET;[4] the only difference is in the form of the tunnel rates. Note that the bath response time τ_{resp} defined in equation (14) is simply given by $\tau_{resp} = 1/(\Gamma_\Sigma)$, as could have been expected: this is the timescale which characterizes charge relaxation on the SET island.

For a normal-metal SET, in the case where both junctions have a conductance ge^2/h and equal capacitances, the tunnel rates are given by

$$\Gamma_\pm(E) = \frac{g(E_\pm + E)}{h}[1 + n_B(E_\pm + E)], \tag{19}$$

where n_B is the Bose–Einstein distribution function and $E_\pm$ is the gain of electrostatic energy associated with each tunnelling process

$$E_+ = eV_{ds}/2 - 2E_C(1/2 - \mathcal{N}). \tag{20a}$$

$$E_- = eV_{ds}/2 + 2E_C(1/2 - \mathcal{N}). \tag{20b}$$

---

[4] Note that there is a difference between a normal-metal SET and a Coulomb-blockaded quantum dot: the former system has a vanishing single-particle level spacing, while the latter system has a large single-particle level spacing. As a result, the tunnelling rates and back-action are quite different.

As a result, at zero physical temperature in the SET, the effective temperature and back-action damping are given by

$$k_B T_{eff} = p_0 p_1 e V_{ds}, \tag{21a}$$

$$m\gamma = A^2 \cdot \frac{h}{g(eV_{ds})^2}, \tag{21b}$$

where $p_0 = \Gamma_-/\Gamma_\Sigma$ is the probability of having $n = 0$ and $p_1 = 1 - p_0$ is the probability of having $n = 1$. For a fixed V_{ds}, the damping is constant, while the effective temperature reaches its maximum $eV_{ds}/4k_B$ at the point of maximum current, $\mathcal{N} = 1/2$. Note these results are in agreement with [9, 12], which treats the SET–oscillator system using a generalized master equation.

Turning to the case of an SSET with identical junctions, the quasi-particle tunnelling rates are now given by

$$\Gamma_\pm = I_{SS}[(E_\pm + E)/e][1 + n_B(E_\pm + E)]. \tag{22}$$

Here, $I_{SS}(V)$ is the usual I–V characteristic of an superconductor–insulator–superconductor (SIS) junction [29]: there is no current until $V = 2\Delta/e$, after which there is an abrupt rise. In the usual case where there is some inelastic scattering in the superconductor, this discontinuity in the I–V curve is smeared out over a voltage $h/(e \cdot \tau_{QP}) \ll \Delta/e$, where τ_{QP} is the quasi-particle lifetime in the superconductor [30].[5] Note that the threshold voltage for quasi-particle-sequential tunnelling is $V_{DS} = 4\Delta$, as one needs to create four quasi-particles to transfer a charge e from left to right. To compare against the normal SET case, we further specialize to the case where $\mathcal{N} = 1/2$; this gives a maximum current. We now have for both normal and SSET's that $\Gamma_+ = \Gamma_- \equiv \Gamma$, and

$$k_B T_{eff} = \frac{\Gamma}{2 \cdot \partial_E \Gamma}, \tag{23a}$$

$$m\gamma = A^2 \frac{\partial_E \Gamma}{4\Gamma^2}. \tag{23b}$$

For drain–source voltages much larger than $4\Delta/e$, the tunnel rates for the quasi-particles will be almost identical to that for normal electrons, and the back-action will be almost identical to that in a normal SET at a similar voltage. However, for $eV_{DS} \sim 4\Delta$, the sharp rise of the SIS current–voltage characteristic will lead to stronger back-action in the superconducting case. One finds that $\partial_E \Gamma$ will be larger than in the normal state case by a large factor $\Delta \tau_{QP}/h$. Thus, one has

$$k_B T_{eff} \sim \frac{h}{\tau_{QP}}, \tag{24a}$$

$$m\gamma \sim A^2 \frac{\tau_{QP}}{\Delta}. \tag{24b}$$

---

[5] Note that environmental voltage fluctuations in the SET will have a similar effect of smearing out the energy dependence of the quasi-particle tunnel rates, and can also be parametrized by τ_{QP}.
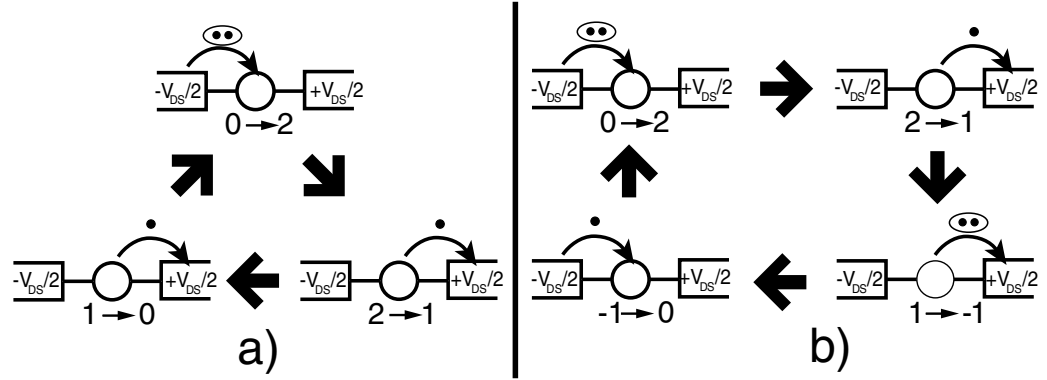
Figure 1. (a) Schematic representation of the JQP process, showing each of the three charge transfer steps. (b) Schematic representation of the DJQP process.

Thus, near threshold, quasi-particle-sequential tunnelling can lead to very low-effective temperatures and high-damping rates. This behaviour is entirely due to the sharp dependence of the quasi-particle tunnelling rates on energy, and is limited by this sharpness. Note that unlike a normal SET or a tunnel junction NEMS, the scale of T_{eff} here is not simply set by the drain–source voltage.

4. Back-action of incoherent Cooper-pair tunnelling

4.1. JQP process

We now examine the back-action of incoherent Cooper-pair tunnelling processes in an SSET. The simplest of such process is the JQP resonance, a transport cycle which has been studied extensively in the context of superconducting qubits [16, 17, 31, 32]. The first step of a JQP cycle involves a Cooper-pair tunnelling through one junction of the SET, changing the charge state of the SET island by two electrons. This is followed by two-quasi-particle tunnelling events through the other junction which return the SET island to its initial charge state; the cycle then repeats (see figure 1(a)). Unlike sequential tunnelling (of either electrons or quasi-particles), incoherent Cooper-pair tunnelling is a quantum resonant process; as such, its back-action will have unique signatures.

For definiteness, we focus on a JQP resonance where a Cooper pair first tunnels onto the island from the left, taking the island charge from $n = 0$ to $n = 2$. We then have a quasi-particle tunnelling event involving the right lead, taking the island charge from $n = 2$ to $n = 1$ (described by a rate Γ_a). Finally, another quasi-particle tunnelling occurs in the right lead, taking $n = 1$ to $n = 0$ (described by a rate Γ_b). There are three important energy scales here: δ, the detuning of the Cooper-pair resonance, and $E_a(E_b)$, the amount of energy driving the quasi-particle event $\Gamma_a(\Gamma_b)$. In the case of symmetric SSET junctions, these energies are given simply by

$$\delta = E_{\text{final}} - E_{\text{initial}} = 4E_C(1 - \mathcal{N}) - eV_{DS}, \tag{25a}$$

$$E_a = 2E_C(3/2 - \mathcal{N}) + eV_{DS}/2 = \delta/2 + eV_{DS} + E_C, \tag{25b}$$

$$E_b = 2E_C(1/2 - \mathcal{N}) + eV_{DS}/2 = \delta/2 + eV_{DS} - E_C. \tag{25c}$$

The modification for non-symmetric junctions is straightforward (see e.g. [33]). The quasi-particle tunnelling rates Γ_a and Γ_b are determined from E_a, E_b and equation (22). Note that as $E_a > E_b$, one always has $\Gamma_a > \Gamma_b$.

To calculate the current near the JQP feature, the standard approach is to calculate the equation of motion for a reduced density matrix describing the SSET island charge; this is done to the lowest non-vanishing order in perturbation theory in tunnelling of the junctions [16]. The approximation here is that the tunnelling is weak, which requires the dimensionless conductance g of the junctions to be much smaller than 2π (we consider the case where both junctions have equal conductances for simplicity). This density-matrix approach can be extended to calculate the quantum charge noise of the island, as discussed in [28]. One again, uses the 'qubits as spectrometer' idea discussed in the previous section and studies a system where the SSET island is coupled to a TLS. In complete analogy to the calculation for the charge noise of sequential tunnelling [23], the weak-coupling, long time dynamics of this system, evaluated for different TLS-splitting frequencies, yields the quantum-noise spectrum of $\hat{n}$.

In what follows, we present results for the transport and noise properties for the JQP cycle obtained from this approach. Three main interesting effects are found: (i) JQP can lead to an extremely low-effective temperature, meaning that it can be used for active cooling; (ii) JQP can lead to negative-damping effects; the resulting instability leads to an interesting regime of strong electromechanical feedback (to be described in detail in section 5); (iii) JQP can be used to reach the quantum limit of position detection within a factor of two.

The current for the JQP process is given by [16]

$$I[\mathcal{N}, V_{ds}] = 2e \frac{E_J^2 \Gamma_a}{4\delta^2 + (\hbar\Gamma_a)^2 + E_J^2(2 + \Gamma_a/\Gamma_b)}. \tag{26}$$

Here, $E_J = g\Delta/8$ is the Josephson energy which sets the strength of coherent Cooper-pair tunnelling. Note that both Γ_a and Γ_b in the above equation depend only weakly on $\mathcal{N}$ and V_{DS} near the JQP resonance; the main dependence of the current on these parameters is through δ, the energy detuning of the Cooper-pair resonance. To obtain a heuristic understanding of the JQP cycle, it is useful to consider equation (26) in the limit of a small $E_J/(\hbar\Gamma_a)$; this limit is often approached in real experiments. In this limit, Cooper-pair tunnelling is the limiting step of the JQP cycle, and one finds the simple result that I is $2e$ times the incoherent Cooper-pair tunnelling rate from the charge state $n = 0$ to $n = 2$:

$$I = 2e \times \Gamma_{CPT}(\delta) = 2e \times \left(\frac{E_J}{2}\right)^2 \frac{\Gamma_a}{\delta^2 + (\hbar\Gamma_a/2)^2}. \tag{27}$$

The incoherent Cooper-pair tunnelling rate has the usual form expected from Fermi's golden rule: a transition matrix element squared (i.e. $(E_J/2)^2$) times a density of states. Here, the density of states is that of the final $n = 2$ charge state, which is lifetime broadened by the quasi-particle transition Γ_a.

We turn now to the back-action of the JQP process. For simplicity, we will focus on operating points near the centre of the JQP resonance, and make use of the smallness of the dimensionless conductance g. In this regime, one can safely neglect the quasi-particle contributions to back-action damping (i.e. $\partial_E\Gamma_a$, $\partial_E\Gamma_b$), as they are higher order in g. The dominant contribution to back-action damping will instead arise from the oscillator's ability to modify the condition for

resonance; as we will discuss, this is in complete analogy to damping in a number of different quantum resonant systems. The neglect of quasi-particle damping will allow us to derive some simple analytic expressions characterizing the back-action.

In the usual limit of a small oscillator frequency (i.e. $\Omega \ll \Gamma_a, \Gamma_b, E_J$), the back-action of an SSET biased near the JQP resonance is described by

$$k_B T_{eff} = \frac{(\hbar \Gamma_a)^2 + 4\delta^2}{16\delta}, \tag{28a}$$

$$\frac{m\gamma}{A^2} = 16\delta \cdot \frac{E_J^2 \Gamma_a}{\Gamma_b^2} \left(\frac{4\delta^2 + c_1(\hbar\Gamma_a)^2 + c_2 E_J^2}{(4\delta^2 + (\hbar\Gamma_a)^2 + c_3 E_J^2)^3} \right), \tag{28b}$$

$$\tau_{resp} \equiv \frac{-m\gamma}{\Delta k} = \frac{\Gamma_a}{\Gamma_b (\Gamma_a + 2\Gamma_b)} \cdot \frac{4\delta^2 + c_1(\hbar\Gamma_a)^2 + c_2 E_J^2}{4\delta^2 + (\hbar\Gamma_a)^2 + c_3 E_J^2}, \tag{28c}$$

where the dimensionless coefficients c_1, c_2 and c_3 are determined by the asymmetry between the two quasi-particle tunnel rates

$$c_1 = 1 + 4\frac{\Gamma_b}{\Gamma_a} + 8\left(\frac{\Gamma_b}{\Gamma_a}\right)^2, \tag{29a}$$

$$c_2 = 1 + 4\frac{\Gamma_b}{\Gamma_a} + 4\left(\frac{\Gamma_b}{\Gamma_a}\right)^2, \tag{29b}$$

$$c_3 = 2 + \frac{\Gamma_a}{\Gamma_b}. \tag{29c}$$

Note that the above expressions are valid for *arbitrary* ratios of E_J/Γ_a and Γ_a/Γ_b.

Several comments are in order. Firstly, note that whenever the detuning of the Cooper-pair resonance is negative (i.e. $\delta < 0$), both T_{eff} and δ become negative. This behaviour has a simple physical interpretation [28]. From equation (25a), we see that $\delta > 0$ means that V_{DS} is *smaller* than what is needed to have the Cooper pairs on resonance. In this case, if the tunnelling Cooper pairs can absorb energy from the oscillator they can move closer to resonance, while if they emit energy to the oscillator, they will move further away from resonance. The net result is that the SSET prefers to *absorb* energy from the oscillator, which implies both $\gamma > 0$, $T_{eff} > 0$; this is the same behaviour exhibited by an equilibrium bath. In contrast, when $\delta < 0$, the situation is reversed. V_{DS} is now larger than what is needed to have the Cooper pairs on resonance, and the SSET prefers to *emit* energy to the oscillator in order to move the Cooper pairs closer to resonance. This is the meaning of negative damping and negative temperature: our effective bath (i.e. the SSET) prefers to *excite* the oscillator rather than to absorb energy from it. Using equation (10), we see that the effect of negative damping is to *reduce* the total damping compared to that provided by the equilibrium bath and *increase* the oscillator temperature. For $\gamma + \gamma_0 < 0$, the total damping of the oscillator becomes negative, and we enter an interesting unstable regime. The properties of this regime are the subject of section 5.

The fact that the sign of γ and T_{eff} change as we tune the detuning δ through the resonance is a generic feature of the noise properties of a number of different resonant systems. For example,

identical effects occur in an optical Fabry-Perot cavity where one mirror is flexible [19]–[21]. If such a cavity is driven by laser light which is slightly detuned from the frequency of the cavity, the resulting 'bath' of cavity photons will both damp and heat the mirror. The detuning parameter in this case is $\delta = \hbar(\omega_{\text{cavity}} - \omega_{\text{laser}})$; when $\delta < 0$, photons from the laser can become resonant with the cavity if they give up energy to the mirror, and one gets negative damping. This analogy can in fact be taken further: *the effective temperature for the optical cavity system is identical to the expression found for JQP*, cf equation (28a) [21]. For the JQP process, T_{eff} is set by the detuning δ and the quasi-particle rate Γ_a; Γ_a is the inverse lifetime of the resonant $n = 2$ charge state. The expression for the optical cavity system is identical, with Γ_a being replaced by the inverse lifetime of a photon in the cavity [21]. The correspondence is a direct consequence of the fact that in both cases, the motion of a mechanical degree of freedom modifies a resonance condition.

While the analogy to the optical cavity system is certainly useful, there are some respects in which it is different from JQP case. Consider the expression for the response time τ_{resp} of our effective bath. As expected, τ_{resp} scales as the lifetime of the resonant state (i.e. $1/\Gamma$). More surprising is the fact that τ_{resp} depends on the detuning δ: our effective bath responds slower when we are on resonance. This is in sharp contrast to what is found for the cavity plus mirror system discussed above; there, the response time is always set by the cavity ring-down time, regardless of detuning [19]–[21].

Finally, we wish to emphasize the smallness of T_{eff} for the JQP process: unlike the normal metal SET or tunnel junction, the effective temperature here is not set by the source–drain voltage, but rather by a much smaller scale, Γ_a. As with the case of sequential-quasi-particle tunnelling, we see that the T_{eff} of a mesoscopic conductor is by no means always set by the drain–source voltage. The effective temperature is rather a measure of the asymmetry between energy absorption and emission. In the present case, the smallness of Γ_a means that incoherent Cooper-pair tunnelling can be used for substantial cooling of the resonator when $\delta > 0$; we give numerical estimates of the magnitude of this cooling effect in section 4.3.

4.2. DJQP back-action

We now turn to the back-action of a slightly more complex incoherent Cooper-pair tunnelling process, the DJQP resonance. This cycle consists of two incoherent Cooper-pair tunnelling events in series, one in each junction (see figure 1(b)); its back-action properties (in the context of qubit measurements) were studied in [28]. The DJQP process is of interest as it occurs at a smaller drain–source voltage in the SET than the JQP process; as we will see, it also has more pronounced back-action and can have a greater cooling effect.

For definiteness, we consider the following cycle: (i) Cooper-pair tunnels from left, taking the island charge from $n = 0$ to $n = 2$; (ii) quasi-particle tunnels from island to right lead, taking $n = 2$ to $n = 1$; (c) a Cooper-pair tunnels from the island to the right lead, taking $n = 1$ to $n = -1$; (d) a quasi-particle tunnels onto the island from the left lead, taking $n = -1$ to $n = 0$. At this stage, the cycle repeats. Note that there are two Cooper-pair tunnelling events (one in each junction) and two quasi-particle tunnelling events (one in each junction). We denote the first quasi-particle transition rate ($n = 2$ to $n = 1$) by Γ_a and the second by Γ_b. We also denote the first Cooper-pair transition ($n = 0$ to $n = 2$) as 'A' and the second transition ($n = 1$ to $n = -1$) as

'B'. As with the JQP process, we have to worry about the following voltage-dependent energies:

$$\delta_A = 4E_C(1 - \mathcal{N}) - eV_{DS}, \tag{30a}$$

$$\delta_B = -4E_C(0 - \mathcal{N}) - eV_{DS}, \tag{30b}$$

$$E_a = 2E_C(3/2 - \mathcal{N}) + eV_{DS}/2, \tag{30c}$$

$$E_b = -2E_C(-1/2 - \mathcal{N}) + eV_{DS}/2. \tag{30d}$$

Here, δ_A, δ_B are the detunings of the two Cooper-pair transitions, and E_a and E_b are the energies driving the two quasi-particle transitions. The rates Γ_a and Γ_b of these quasi-particle transitions are related to the corresponding driving energies by equation (22) as before. Note that the centre of the DJQP resonance (where both δ_A and δ_B are 0) occurs when both $\mathcal{N} = 1/2$ and $eV_{ds} = 2E_C$.

An density-matrix approach identical to that used for the JQP may be used to describe the transport and noise properties of the DJQP. While this technique is valid for arbitrary ratios Γ_b/Γ_a and E_J/Γ_a, we will make some additional mild approximations to obtain results that may be easily interpreted. Firstly, we again consider an SSET with identical junctions, and note that at the centre of the DJQP resonance, $\Gamma_a = \Gamma_b$. As we are interested in the behaviour near the resonance centre, we will take $\Gamma_a = \Gamma_b = \Gamma$ throughout. In addition, we will consider the limit $E_J \ll \Gamma$; this limit is approximately realized in many experiments, and leads to a great simplification in the form of the resulting equations.

In this limit, the Cooper-pair tunnelling is the rate-limiting step in the DJQP cycle; we find that the average current is given by $3e$ times the series addition of the incoherent Cooper-pair tunnelling rates for the 'A' and 'B' transitions

$$I = 3e \times \left(\frac{1}{\Gamma_{CPT}(\delta_A)} + \frac{1}{\Gamma_{CPT}(\delta_B)} \right)^{-1} = \frac{3e}{2} \frac{E_J^2 \Gamma}{(\hbar\Gamma)^2 + 2\delta_A^2 + 2\delta_B^2}. \tag{31}$$

The incoherent Cooper-pair tunnelling rate $\Gamma_{CPT}(\delta)$ is defined in equation (27).

In calculating the back-action for the DJQP process, we again make the assumption that we can ignore the quasi-particle contribution to damping; as discussed, near the resonance, this contribution leads to terms which are higher order in the dimensionless conductance g. For the effective temperature, we again find a remarkably simple result

$$k_B T_{eff} = \left(\frac{1}{k_B T_{eff,A}} + \frac{1}{k_B T_{eff,B}} \right)^{-1} = \left(\frac{16\delta_A}{(\hbar\Gamma)^2 + 4\delta_A^2} + \frac{16\delta_B}{(\hbar\Gamma)^2 + 4\delta_B^2} \right)^{-1}$$

$$= \frac{[(\hbar\Gamma)^2 + 4\delta_A^2][(\hbar\Gamma)^2 + 4\delta_B^2]}{16[\delta_A + \delta_B][(\hbar\Gamma)^2 + 4\delta_A\delta_B]}. \tag{32}$$

We see that the effective temperature for the DJQP process (in the small E_J limit) is simply given by the series addition of the effective temperature for each individual Cooper-pair resonance; the scale for the minimum effective temperature is again set by Γ (i.e. the lifetime of each of the

two resonant states). The equation for the back-action damping γ is slightly more complicated:

$$\frac{m\gamma}{A^2} = 2\frac{\delta_A + \delta_B}{E_J^2 \Gamma} \left(\frac{[(\hbar\Gamma)^2 + 4\delta_A^2][(\hbar\Gamma)^2 + 4\delta_B^2][(\hbar\Gamma)^2 + 4\delta_A\delta_B]}{[(\hbar\Gamma)^2 + 2\delta_A^2 + 2\delta_B^2]^3} \right). \tag{33}$$

Similar to the situation with JQP, the effective temperature (and damping) can become negative if the *net* preference of the two resonances is to emit energy to the oscillator (i.e. the series addition of $T_{eff,A}$ and $T_{eff,B}$ must be negative). To see exactly where negative damping and temperature occur in terms of SSET operating points (i.e. V_{ds} and $\mathcal{N}$), it is useful to re-write the expression for T_{eff}. We define:

$$4E_C\mathcal{N} = 4E_C(1/2 + \delta\mathcal{N}) = 2E_C + \Delta_\mathcal{N}, \tag{34a}$$

$$eV_{DS} = 2E_C + e\delta V_{DS} = 2E_C + \Delta_V, \tag{34b}$$

where $\Delta_\mathcal{N}$ and Δ_V represent the energy detuning that result when we move, respectively, $\mathcal{N}$ or V_{DS} from the centre of the resonance. With this notation, we have:

$$k_B T_{eff} = \frac{1}{-32\Delta_V} \cdot \frac{[\Gamma^2 + 4(\Delta_V + \Delta_\mathcal{N})^2][\Gamma^2 + 4(\Delta_V - \Delta_\mathcal{N})^2]}{\Gamma^2 + 4[(\Delta_V)^2 - (\Delta_\mathcal{N})^2]}. \tag{35}$$

For small detunings from the centre of the resonance (Δ_V, $\Delta_\mathcal{N} \ll \Gamma$), we see that the sign of the effective temperature is completely determined by the value of the drain–source voltage. If V_{DS} is set to be below the centre of the DJQP resonance, Δ_V is negative, and hence both T_{eff} and the damping γ are positive. In this case, the net preference of the two resonances is to absorb energy from the oscillator. In contrast, if the drain–source voltage is tuned to be higher than resonance, we get both negative temperature and negative damping. Now, the DJQP process can be brought closer to resonance by *emitting* energy to the oscillator. Finally, note if the drain–source voltage is exactly at the centre of the resonance (i.e. $\Delta_V = 0$), T_{eff} tends to infinity, meaning that there is no damping and no asymmetry between absorption and emission; this holds regardless of how much one moves the gate voltage $\mathcal{N}$ off-resonance. In this special case, one Cooper-pair transition always prefers to absorb energy, the other to emit; the net result is no preference between absorption and emission. In figure 2, we show a contour plot of T_{eff} for DJQP using typical device parameters and compare it against a plot of the current.

It is instructive to compare the magnitude of detector-induced damping for the JQP and DJQP processes in the small E_J limit we considered. In both cases, the minimum value of $|T_{eff}|$ is $\propto \Gamma$, where Γ is the quasi-particle tunnelling rate. However, the corresponding damping will be much larger in magnitude for DJQP versus JQP: comparing equations (28b) and (33), we see that the back-action damping in the DJQP case is enhanced over that at JQP by a large factor $(\Gamma/E_J)^4$. The reason for this is simple to understand, once we recall that $\gamma \propto S_n(0)/T_{eff}$, where $S_n(0)$ is the zero-frequency charge noise of the SSET island. For both JQP and DJQP, this noise has a telegraph-noise form in the small E_J limit. For JQP, we have effective telegraph noise between the $n = 0$ and $n = 2$ charge states, where one rate (the quasi-particle transition rate Γ) is much larger than the other (the incoherent Cooper-pair tunnelling rate Γ_{CPT}). As a result, $S_n(0) \propto \Gamma_{CPT}/\Gamma^2$. In contrast, for DJQP, we have effective telegraph noise between the $n = 0$ and $n = 1$ charge states; the two telegraph rates are both incoherent Cooper-pair tunnelling rates (i.e. the 'A' and 'B' transitions) and are roughly equal. In this case, $S_n(0) \propto 1/\Gamma_{CPT}$. Thus, as
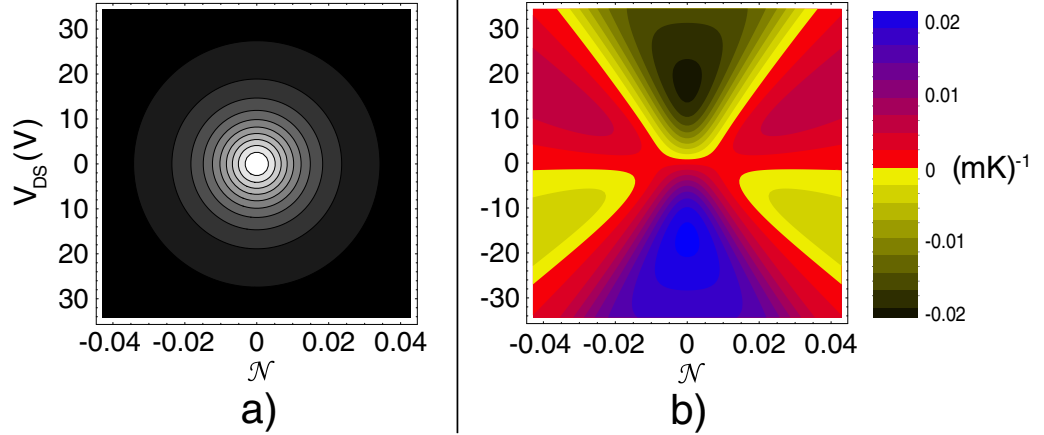
Figure 2. (a) Contour plot (with equally spaced contours) of current near DJQP resonance, as a function of gate-voltage detuning ($\Delta\mathcal{N} = \mathcal{N} - 1/2$) and drain–source voltage detuning ($\Delta V_{DS} = V_{DS} - 2E_C/e$) from the resonance centre. We have chosen typical SSET parameters $\Delta = E_C = 0.2\,\text{meV}$ and $g = 0.2$. (b) Contour plot of $(T_{osc})^{-1}$, the inverse of the oscillator's temperature (cf equation (10)), for the same range of ΔV_{DS} and $\Delta\mathcal{N}$. We have taken typical oscillator parameters $\Omega/(2\pi) = 27\,\text{MHz}$, $Q_0 = 10^4$ (i.e. intrinsic oscillator quality factor), $d = 300\,\text{nm}$ (i.e. oscillator–SET island distance), $C_{osc} = 0.1C_\Sigma$ and $V_{osc} = 10\,\text{V}$ (cf equation (17)); we have also chosen a bath temperature of $T_0 = 500\,\text{mK}$. Yellow colour indicates unstable regions where the oscillator temperature is negative. In the regions of cooling (blue), the lowest achievable oscillator temperature is less than $50\,\text{mK}$, a factor of ten lower than the oscillator's temperature at zero coupling to the SET.

both processes have similar effective temperatures, the enhanced charge noise of DJQP explains its enhanced damping. This enhancement of back-action damping should make it easier to see back-action effects of DJQP in an experiment.

Finally, consider the response time τ_{resp} of the effective bath presented by DJQP; it is given by

$$\frac{1}{\tau_{resp}} = \Gamma_{CPT}(\delta_A) + \Gamma_{CPT}(\delta_B) = \frac{2E_J^2}{\hbar^2\Gamma} \times \frac{(\hbar\Gamma)^2[(\hbar\Gamma)^2 + 2\delta_A^2 + 2\delta_B^2]}{[(\hbar\Gamma)^2 + 4\delta_A^2][(\hbar\Gamma)^2 + 4\delta_B^2]}. \tag{36}$$

The average response rate, $1/\tau_{rep}$, is simply given by the sum of the rates of the two Cooper-pair tunnelling events in the cycle. In the small E_J limit we are considering, this timescale is much longer than what was found for JQP (cf equation (28c)), where one always had $\tau_{resp} \sim 1/\Gamma$.

As a final note, we should remark that none of the approximations used here (small E_J, no quasi-particle contribution to damping) are necessary to the method used. We have made these approximations only so that we could give a clear heuristic picture of the physics underlying the back-action effects found.

4.3. Typical cooling temperatures

Equation (10) tells us that if the back-action damping dominates the intrinsic, non-back-action damping of the oscillator (i.e. $\gamma \gg \gamma_0$), then it should be possible to cool the oscillator to the effective temperature of the SET, even if this is much lower than T_0 (i.e. the temperature of the oscillator when it is decoupled from the SET). To achieve $\gamma \gg \gamma_0$, one should start with an oscillator with a high-intrinsic quality factor, and engineer structures where the SET–oscillator coupling is relatively strong (e.g. have the SET island be in close proximity to the oscillator). Note that this condition does not imply any violation of the weak-coupling assumptions of our treatment: it is entirely possible to have the coupling A weak enough that linear response is still valid, yet strong enough that $\gamma \gg \gamma_0$.

To give an idea of the kind of cooling that should be achievable using incoherent Cooper-pair tunnelling, it is useful to give some numerical estimates using typical SET parameters. We assume $E_C = \Delta = 0.2 \, \text{meV}$, in agreement with the devices used in [34]. For the JQP, we saw that the minimum possible positive value of T_{eff} was given by $\Gamma_a/4$. By choosing $V_{DS} = 2\Delta + E_C$ (the threshold voltage for the JQP process), we found that for these parameters

$$T_{eff}|_{min} \simeq g \times 350 \, \text{mK}. \tag{37}$$

Thus, for $g = 0.2$ (i.e. a junction resistance of $130 \, \text{k}\Omega$), the minimum effective temperature is approximately $70 \, \text{mK}$; again, this is the minimum temperature we could cool our oscillator to using the JQP process. Note that this T_{eff} is much lower than the scale set by the voltage: $eV_{DS}/k_B \simeq 7.0 \, \text{K}$.

Turning to the DJQP, and now assuming the typical condition $E_J < \Gamma$, we see from equation (32) that the minimum possible positive value of T_{eff} is $\Gamma/8$, a full factor of two smaller than for the JQP process. If we again take $E_C = \Delta = 0.2 \, \text{meV}$, we found

$$T_{eff}|_{min} \simeq g \times 125 \, \text{mK}. \tag{38}$$

For systems with $E_J < \Gamma$, cooling should be much easier to achieve using DJQP. Not only is the T_{eff} lower, but, as already discussed, the back-action damping due to DJQP is larger than that of JQP by the large factor $(\Gamma/E_J)^4$.

As a final caveat, the above estimates assume that the only source of broadening of the Cooper-pair tunnelling resonances is quasi-particle tunnelling. In reality, additional effects could further broaden these resonances and increase the minimum achievable temperature. Perhaps the most important of these will be voltage fluctuations associated with the environmental impedance seen by the SET island. These effects will ultimately limit how much one can lower T_{eff} by simply lowering g.

4.4. Quantum-limited measurement with incoherent Cooper-particle tunnelling

There is an additional important point that needs to be made about incoherent Cooper-pair tunnelling processes: unlike sequential tunnelling in a normal SET, these processes may be used to do near quantum-limited displacement detection [28]. As discussed extensively in [22], reaching the quantum limit requires a detector which has a minimal amount of back-action noise relative to the amount of information it provides. The measure of this relative back-action is the noise temperature T_N of the detector, which gives a measure of how much noise is added to the

signal by the detector. The quantum limit is that $k_B T_N$ cannot be any smaller than $\hbar\Omega/2$, where Ω is the oscillator's frequency [35]. We are interested in the usual limit where the detector noise correlators are frequency independent on frequency scales relevant to the oscillator (i.e. Ω, γ). After optimizing the strength of the coupling A (to balance back-action and intrinsic shot noise contributions to the total noise), one has [22]

$$\chi \equiv \frac{k_B T_N}{\hbar\Omega/2} = \sqrt{\frac{4S_I(0)S_F(0)}{(\hbar\,\mathrm{d}I/\mathrm{d}x)^2}} \geqslant 1. \tag{39}$$

Here, $S_F = A^2 S_n$ is the back-action force noise spectrum of the detector, S_I is the zero frequency current noise of the SSET and $\mathrm{d}I/\mathrm{d}x = -(\mathrm{d}I/\mathrm{d}\mathcal{N})\frac{2A}{E_C}$ is the gain of our detector: how strongly does the average current respond to changes in the oscillator's position.

Thus, achieving the quantum limit of displacement detection requires that χ approaches one[6]. For a normal-metal SET in the sequential-tunnelling regime, χ is proportional to $1/g^2$, where g is the dimensionless conductance of the junctions. By assumption, g is a small parameter—this is what allows us to use perturbation theory in the tunnelling! One thus has that sequential tunnelling in a normal SET is far from being at the quantum limit; there is considerable excess back-action noise, far beyond what is required by quantum mechanics. In contrast, for JQP and DJQP, χ is of the order 1 and is independent of g [28]. Using the same density-matrix approach used to calculate the charge noise, one can calculate the zero frequency current noise of both JQP and DJQP [28, 32, 36]. Shown in figure 3 is the reduced noise temperature χ for JQP and DJQP, evaluated as a function of the ratio E_J/Γ, and for a bias point which yields a maximum gain. Note that the ratio E_J/Γ can in principle be controlled, if one can control the ratio of E_C to Δ when fabricating the SET. We see when that $E_J \simeq \Gamma$, both DJQP and JQP come close to reaching the quantum limit, with the DJQP process doing slightly better. In the more usual case, where $E_J \ll \Gamma$, the JQP process is much better at approaching the quantum limit than the DJQP process; this is because of the relative suppression of charge noise associated with JQP when $E_J \ll \Gamma$.

5. Negative damping and strong electromechanical feedback

In this last section, we describe in more detail the interesting negative-damping instability that can be brought about by incoherent Cooper-pair tunnelling in an SET plus mechanical resonator system. As discussed, the negative back-action damping associated with either the JQP or DJQP transport cycles can, for a sufficiently strong coupling, drive both the *total* oscillator damping and its temperature T_{osc} (as given by equation (10)) below zero (e.g. see the yellow regions in figure 2(b)). In this regime, the SET will continually dump energy into the oscillator, causing the amplitude of the oscillator's motion to continually increase. Eventually, this amplitude will become so large that there will be an effective strong coupling between the oscillator and the SET—the motion of the oscillator will strongly effect the dynamics of the SET. In this regime, the weak coupling approximations we have been making clearly breakdown. We nonetheless wish to describe the properties of the eventual stationary state achieved in this regime. Note that

---

[6] Note that if our detector was used to do a weak QND measurement of a qubit, $1/\chi^2$ represents the ratio between the rate at which information is acquired by the measured versus the back-action dephasing rate.
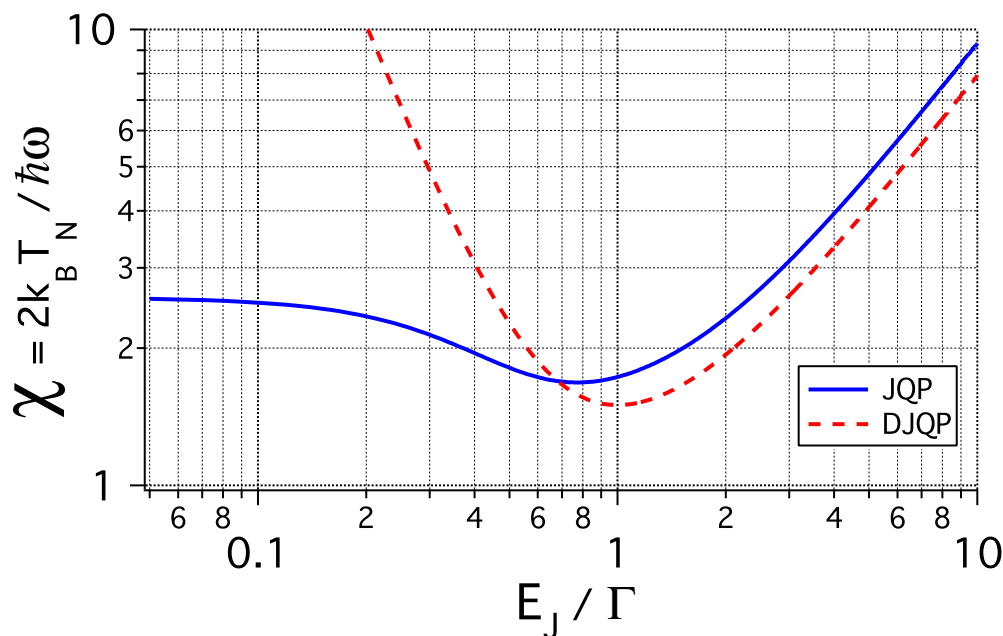
Figure 3. Noise temperature for the JQP and DJQP processes (scaled by $\hbar\Omega/2$) versus E_J/Γ, where E_J is the Josephson energy and Γ is the quasi-particle tunnelling rate. We have assumed an optimal choice of coupling strength A, identical SET junctions and that both quasi-particle tunnelling rates in each cycle are the same.

such negative-damping instabilities are also well known in the analogous optical cavity system [37]–[39].

To deal with the feedback occurring in this effective strong coupling regime, we will make the usual simplifying assumption that the oscillator is much slower than the SET: $\Omega \ll \Gamma, \Gamma_{CPT}$; this condition is usually more than satisfied in experiment. We can then make use of this separation of timescales in a manner somewhat analogous to the usual Born–Oppenheimer approximation. As in our original weak-coupling description, at each instant in time, the SET acts as an effective thermal bath on the oscillator and is characterized by a fluctuating back-action force with spectral density $S_{\delta f}$ and a damping rate γ; the oscillator is thus still described by the Langevin equation equation (3). Now, however, the parameters of the bath will depend on the instantaneous position of the oscillator: this is how we deal with the strong-coupling aspect of the problem. Thus, the spectral density of the back-action force $\delta f(t)$ appearing in equation (3) will be x-dependent (i.e. $S_{\delta f} = S_{\delta f}[x]$), as will the damping coefficient γ (i.e. $\gamma = \gamma[x]$). The x dependence of both these quantities arises completely through their dependence on the SET dimensionless gate voltage $\mathcal{N}$; we can absorb the coupling Hamiltonian of equation (1) into the SET charging energy Hamiltonian (cf equation (15)) by writing

$$\mathcal{N}[x] = \mathcal{N}[0] + \frac{A}{2E_C}x = \frac{C_g V_g}{e} + \frac{A}{2E_C}x. \tag{40}$$

Again, the key assumption here is that the SET response to changes in x is much faster than the evolution of x itself.

As we show in what follows, the net result of this approach is that, we may describe our coupled system with a classical Fokker–Planck equation where *both* the diffusion and damping constants have an explicit x dependence. Heuristically, for large oscillator amplitude, the Cooper-pair detuning δ and hence the back-action damping will depend on the position of the oscillator; in the unstable regime of interest, the stationary state of the oscillator will correspond to an amplitude of oscillation so large that the oscillator experiences equal amounts of positive and negative damping during one period of its motion. More quantitatively, we find that the stationary state of oscillator is naturally characterized by an *energy-dependent temperature*; for a variety of regimes, the energy distribution of the oscillator is a Gaussian and hence highly non-thermal. Note that a similar approach to potential strong-feedback behaviour was used in [11]; however, the particular NEMS studied in that work did not exhibit any negative damping, and thus there was no effective strong-coupling regime.

Our starting point is thus the Langevin equation of equation (3) with x-dependent damping and back-action force terms. As we are interested in the limit where the oscillator is much slower than the source of the back-action noise, we can treat the latter as being white. We may then convert our Langevin equation into a Fokker–Planck equation for the oscillator's phase-space density $w(x, p; t)$ in the usual way [40]; we then obtain

$$\frac{\partial}{\partial t} w = \left[-\frac{p}{m} \frac{\partial}{\partial x} + \frac{\partial}{\partial p} (m\Omega^2 x + (\gamma_0 + \gamma[x]) p) \right] w + (D_0 + D[x]) \frac{\partial^2}{\partial p^2} w. \tag{41}$$

Here, γ_0 is the intrinsic (SET-independent) damping of the oscillator, $D_0 = m\gamma_0 k_B T_0$ describes momentum diffusion due to the equilibrium bath and the x-dependent diffusion constant $D[x]$ is determined from back-action force spectrum

$$D[x] = \tfrac{1}{2} S_{\delta f}[\omega = 0; x] = m \cdot \gamma[x] \cdot k_B T_{eff}[x]. \tag{42}$$

In the case of JQP, $\gamma(x)$ and $T_{eff}[x]$ are given respectively by equations (28*b*) and (28*a*) with the substitution $\mathcal{N} \to \mathcal{N}[x]$; for DJQP, one would use equations (32) and (33). Note that there is no ambiguity in interpreting equation (3) with an x-dependent back-action noise spectrum: both the Ito and Stratonovitch interpretations of this stochastic differential equation yield the same Fokker–Planck equation. Also note that we are neglecting the x dependence of the conservative part of the average back-action force; this is justified in the experimentally relevant limit of a high-intrinsic quality factor Q_0. In this limit, one can have the magnitude of back-action damping comparable or greater than the intrinsic damping of the oscillator, while at the same time have the back-action spring-constant modification Δk much smaller than $m\Omega^2$.

To make further progress, we consider the experimentally relevant weak-damping limit of equation (41) (i.e. $\gamma_0, |\gamma[x]| \ll \Omega$), and follow the approach of Kramers [41] (and more recently, Blanter *et al* [11]). We first re-write x and p in terms of the oscillator's energy E and phase θ ($x = \sqrt{2E/k} \sin \theta$, $p = \sqrt{2mE} \cos \theta$), and then convert equation (41) into an equation for $w(E, \theta)$. Working to lowest order in the dissipative terms (both damping and diffusion), this equation can then be recast as an equation for the oscillator energy distribution $w(E) = \int_0^{2\pi} d\theta \, w(E, \theta)$; one uses the fact that in the absence of any dissipation, $w_0(E, \theta) = w_0(E)/2\pi$. After some algebra, this procedure yields

$$\frac{d}{dt} w(E; t) = \frac{\partial}{\partial E} E \left(\gamma_0 + \gamma(E) + \frac{D_0 + D(E)}{m} \frac{\partial}{\partial E} \right) w(E; t). \tag{43}$$

Institute *of* **Physics** **Φ** DEUTSCHE PHYSIKALISCHE GESELLSCHAFT

The energy-dependent back-action damping and diffusion constants here are defined as:

$$\gamma[E] = 2 \int_0^{2\pi} \frac{d\theta}{2\pi} \gamma(x = \sqrt{2E/k} \sin\theta) \cdot \cos^2\theta, \tag{44}$$

$$D[E] = 2 \int_0^{2\pi} \frac{d\theta}{2\pi} D(x = \sqrt{2E/k} \sin\theta) \cdot \cos^2\theta. \tag{45}$$

As could have been expected, they are given by averaging $\gamma[x]$ and $D[x]$ over the phase of the oscillator at fixed amplitude; what is perhaps more surprising is that one must take a weighted average, with a weighting factor which is proportional to p^2. Note that at $E = 0$, $\gamma(E)$ and $D[E]$ coincide respectively with the back-action damping and diffusion constant in the weak-coupling (i.e. zero feedback) theory.

It is now trivial to solve for the stationary energy distribution of the oscillator. From equation (43), we have

$$w(E)_{stat} = N \exp\left(-\int_0^E \frac{\mathrm{d}E'}{k_B \widetilde{T}_{osc}[E']}\right), \tag{46}$$

where N is a normalization constant, and the energy-dependent effective temperature $\widetilde{T}_{osc}(E)$ is given quite naturally by

$$k_B \widetilde{T}_{osc}(E) \equiv \frac{D_0 + D[E]}{m(\gamma_0 + \gamma[E])}. \tag{47}$$

We see that the stationary state is characterized by a generalized Boltzmann distribution having an energy-dependent effective temperature. In the weak-coupling, no negative-damping case, we can neglect the energy dependence of $k_B \widetilde{T}[E]$, and equation (46) coincides with a thermal distribution and with the results of the weak-coupling theory (cf equation (10)). In the strong-feedback regime of interest, the total damping $(\gamma_0 + \gamma(E))$ is negative at $E = 0$; as we increase E, the motion of the oscillator smears out the back-action contribution to the damping, and for very large E, the total damping tends to $\gamma_0 > 0$. There will thus be a critical $E = E_0$ where $(\gamma_0 + \gamma(E_0))$ will pass through zero. It follows directly from equation (46) that $w(E)$ will have a maximum at E_0; moreover, in the vicinity of E_0, $w(E)$ will look Gaussian

$$w(E)_{stat} \simeq N \exp\left(-\frac{(E - E_0)^2}{2\sigma^2}\right), \tag{48}$$

$$\sigma^2 = \frac{D_0 + D[E_0]}{2m} \left[\frac{\mathrm{d}\gamma}{\mathrm{d}E}\bigg|_{E=E_0}\right]^{-1}. \tag{49}$$

We thus find that in the strong-feedback regime, the oscillator's energy distribution function has a maximum at a non-zero energy, in sharp contrast to an equilibrium distribution. The energy at which the maximum occurs corresponds, as expected, to an oscillator amplitude large enough that the oscillator experiences zero average damping during each period of its motion. The width of the distribution near this maximum is set by *both* the back-action noise and the energy sensitivity of the damping via equation (49).
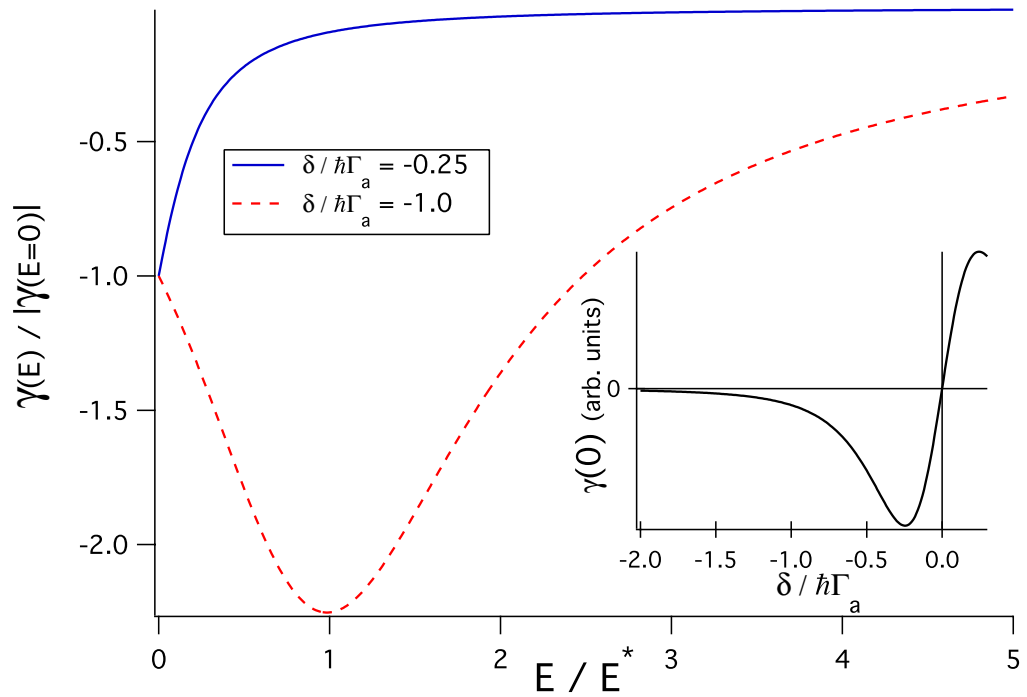
Figure 4. Energy-dependent back-action damping of the JQP process, cf equation (44), plotted as a function of energy, and using SSET parameters identical to those used in figure 2. The characteristic scale for feedback effects, E^*, is given in equation (50). Note that the chosen scaling makes this plot independent of the coupling strength A. The red curve and blue curves correspond to two different Cooper-pair detunings δ (i.e. SSET operating points) as labelled; note that $\gamma(E)$ can have a non-monotonic dependence on energy. The inset shows the dependence of the back-action damping at zero-oscillator energy (cf equation (28b)) on the Cooper-pair detuning.

We now apply the above results, which are quite general, to the specific instability brought on by incoherent Cooper-pair tunnelling. We first consider the case of an oscillator–SSET system operated in the negative-damping regime near the JQP resonance; as usual we consider the limit of small dimensionless junction conductances, and neglect the quasi-particle contribution to the back-action damping. In this limit, all the feedback effects of the oscillator on the SET will be due to the dependence of the Cooper-pair detuning δ (cf equation (25a)) on the oscillator position x. The characteristic energy scale E^* for feedback effects will correspond to an oscillator amplitude large enough that the corresponding oscillations in δ are equal to the resonance width, $\hbar\Gamma_a$. From equations (40) and (25a), one has

$$E^* = \left(\frac{\hbar\Gamma_a}{2A\sqrt{\frac{2}{k}}} \right)^2 . \tag{50}$$

E^* sets the characteristic scale for variations in $\gamma[E]$ and $D[E]$. Shown in the inset of figure 4 is the back-action damping γ at zero energy (i.e. ignoring feedback effects), cf equation (28b), as
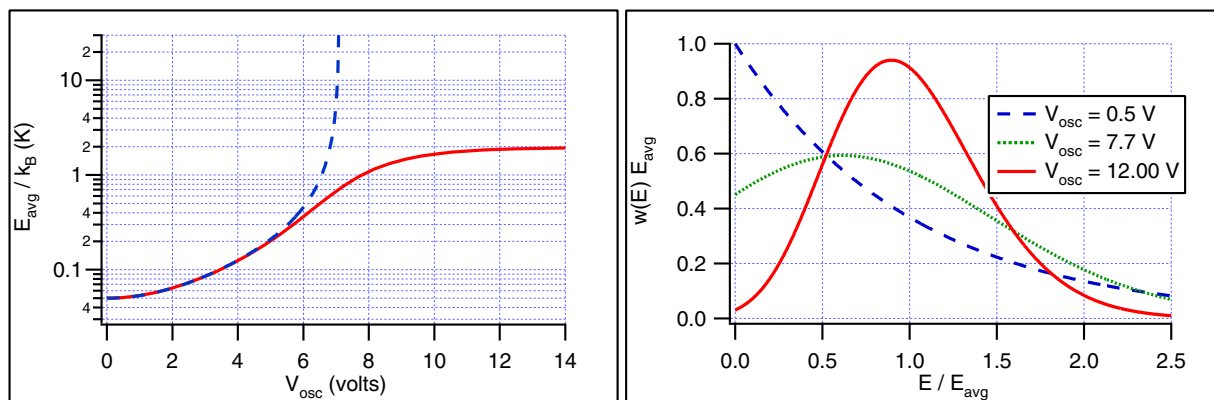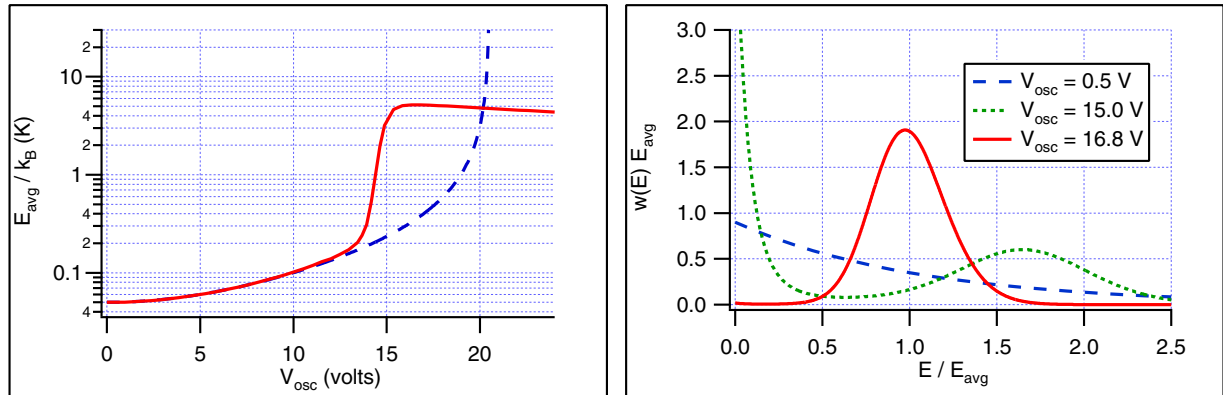
Figure 5. Effects of JQP back-action in the negative-damping regime. We have taken a bath temperature $T_0 = 50$ mK, an intrinsic oscillator quality factor $Q_0 = 10^5$ and an SSET operating point near the JQP resonance which maximizes the effect of the back-action damping ($\delta = -0.25\,\hbar\Gamma_a$). All other parameters are the same as in figure 2. Left panel: average energy of the oscillator E_{avg} as a function of the coupling voltage V_{osc}; the dashed curve is the predictions of the weak-coupling theory, cf equation (10), while the red curve is from the strong-feedback theory. The total oscillator damping becomes negative at $V_{osc} = 7.1$ V]]. Right panel: oscillator energy distribution $w(E)$ as determined by equation (43). As V_{osc} becomes large enough for the strong-feedback effect to take hold, the energy distribution becomes Gaussian-like.

a function of δ. The main plot shows the energy dependence (scaled by E^*) of the damping for two choices of $\delta_0 = \delta[x = 0]$. Note that $\gamma(E)$ can have a non-monotonic dependence on E.

While measuring the full distribution $w(E)$ of the oscillator's energy may be quite difficult, the average oscillator energy E_{avg} can be obtained directly from experiment. In the experiments of LaHaye *et al* [2], this quantity was obtained by extracting $\langle x^2 \rangle$ from the current noise of the SET, and then invoking the equipartition theorem; a similar approach could be used in the strong-feedback regime discussed here[7]. In figure 5(left panel), we plot E_{avg} as a function of the coupling voltage V_{osc}; we use typical device parameters (see figure caption), and choose $\delta = -0.25\,\hbar\Gamma_a$ to maximize $|\gamma(E = 0)|$ (i.e. same as the blue curve in figure 4). For small V_{osc}, the intrinsic damping of the oscillator dominates the back-action damping, and there is no strong-feedback effect. The oscillator is in a thermal state, with a temperature T_{osc} given by equation (10) and $E_{avg} = k_B T_{osc}$. As we increase the coupling voltage, the back-action damping increases in magnitude (i.e. becomes more negative) and $E_{avg} = T_{osc}$ correspondingly increases. At a critical voltage $V_{osc} = 7.1$ V, the total damping becomes negative and the weak-coupling expression for T_{osc} diverges. The strong-feedback effect takes hold here, and we see that average energy of the oscillator remains finite. There is also a corresponding change in the shape of the energy distributions, as can be seen in figure 5(right panel)). Note that for a large range of V_{osc}, E_{avg} remains approximately constant. This is the result of two competing tendencies: increasing V_{osc}

---

[7] As the stationary state is characterized by a flat distribution of the oscillator phase θ, one again has the relation $E_{avg}/k = \langle x^2 \rangle$, as would hold in equilibrium.

Figure 6. Effects of JQP back-action in the negative-damping regime. We use the same parameters as figure 5, but now choose an SSET operating point near the JQP resonance which yields a non-monotonic $\gamma(E)$. ($\delta = -\hbar\Gamma_a$.) Left panel: average energy of the oscillator E_{avg} as a function of the coupling voltage V_{osc}, labelled as in figure 5. Note that the strong-feedback effect sets in at a voltage V_{osc} much lower than what is needed to make the weak-coupling theory diverge. Right panel: oscillator energy distribution $w(E)$ as determined by equation (43).

increases the overall magnitude of the back-action damping, but also increases the sensitivity of the Cooper-pair detuning δ to E.

In figure 6, we plot the same quantities as figure 5, but now for $\delta = -\hbar\Gamma_a$. In this case, the non-monotonic nature of $\gamma(E)$ leads to energy distributions $w(E)$ which have two local maxima. Also note that in this case, the strong-feedback effect sets in well before the weak-coupling expression for T_{osc} diverges. Finally, in figure 7, we plot results for an oscillator–SSET system operated in the negative-back-action damping regime near the DJQP resonance. We have again chosen realistic parameter values (see figure caption). We see that the feedback effect is stronger here; as discussed, this is a consequence of the enhanced back-action damping of DJQP versus JQP. Note that for both the JQP and DJQP strong-feedback results presented here, the maximum amplitude of the oscillator is still much smaller than the oscillator–SET gap d, and the corresponding oscillation of the Cooper-pair detuning is at most of order Γ. Thus, these results do not violate our assumption of a linear coupling Hamiltonian, and do not involve SSET physics far from the JQP or DJQP resonance.

There are a number of other interesting issues related to the strong-feedback regime discussed here. In particular, what are the dynamics of the oscillator's energy in this regime? As the total damping vanishes at the most probable energy E_0, one expects very slow dynamics. How does this then manifest itself in the output noise of the SET? It would also be interesting to investigate systems where the SET is not infinitely fast compared to the oscillator; in this case, one could expect similar kinds of multistability effects found in optical cavity systems [39]. We hope to address these issues in the near future.

6. Conclusions

In this paper, we have discussed various aspects of back-action physics in SET–oscillator NEMS using a quantum-noise approach. In the sequential-tunnelling regime, we derived general
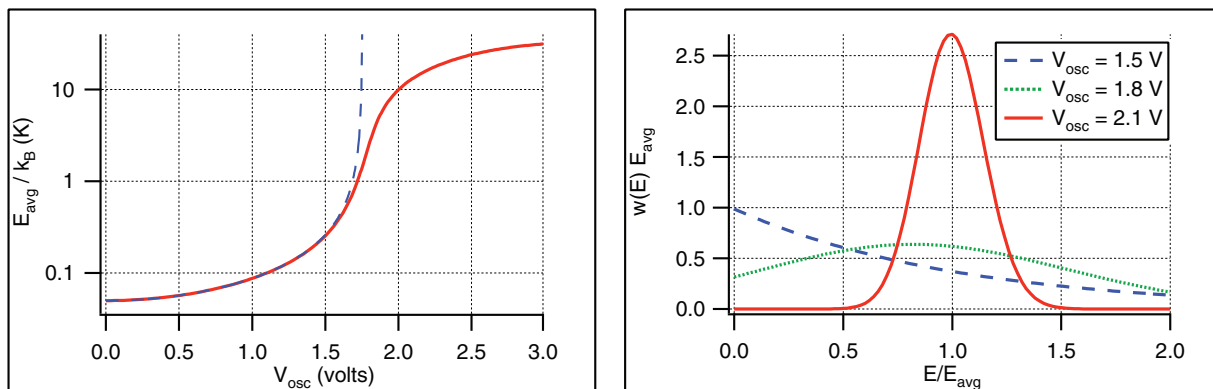
Figure 7. Effects of DJQP back-action in the negative-damping regime. We have taken a bath temperature $T_0 = 50$ mK, an intrinsic oscillator quality factor $Q_0 = 10^4$ and an SSET operating point near the DJQP resonance ($\Delta\mathcal{N} = 0$, $\Delta V = \hbar\Gamma/2$). All other parameters are the same as in figure 2. Left panel: average energy of the oscillator E_{avg} as a function of the coupling voltage V_{osc}; the dashed curve is the predictions of the weak-coupling theory, cf equation (10). The total damping becomes negative when the coupling voltage $V_{osc} = 1.75$ V. Right panel: oscillator energy distribution $w(E)$ as determined by equation (43). At $V_{osc} = 1.5$ V, we still have a thermal distribution; increasing the coupling voltage takes one into the unstable regime and results in an almost Gaussian distribution of energy.

expressions for the effective temperature, damping rate and bath response time that are valid regardless of the particular system (electrons in a normal SET, quasi-particles in an SSET, electrons in a quantum dot). In the regime of incoherent Cooper-pair tunnelling, we described the back-action of both the JQP and DJQP processes, and demonstrated that both could be used for substantial oscillator cooling, as well as near quantum-limited measurement. We also discussed the strong analogy between these processes and an optical cavity with a moveable mirror. Finally, we discussed the regime of strong electromechanical feedback that can arise when the back-action damping becomes negative, and showed that the stationary state in this regime is naturally characterized by an energy-dependent temperature.

Acknowledgments

References

[1] Knobel R G and Cleland A N 2003 *Nature (London)* **424** 291
[2] LaHaye M D, Buu O, Camarota B and Schwab K C 2004 *Science* **304** 74
[3] Mozyrsky D, Martin I and Hastings M B 2004 *Phys. Rev. Lett.* **92** 018303
[4] Clerk A A and Girvin S M 2004 *Phys. Rev.* B **70** 121303

[5] Ruskov R, Schwab K and Korotkov A N 2005 *Phys. Rev.* B **71** 235407
[6] Blencowe M P and Wybourne M N 2000 *Appl. Phys. Lett.* **77** 3845
[7] Zhang Y and Blencowe M P 2002 *J. Appl. Phys.* **91** 4249
[8] Chtchelkatchev N M, Belzig W and Bruder C 2004 *Phys. Rev.* B **70** 193305
[9] Armour A D, Blencowe M P and Zhang Y 2004 *Phys. Rev.* B **69** 125313
[10] Blencowe M P 2004 *Phys. Rep.* **395** 159
[11] Blanter Y M, Usmani O and Nazarov Y V 2004 *Phys. Rev. Lett.* **93** 136802
    Blanter Y M, Usmani O and Nazarov Y V 2005 *Phys. Rev. Lett.* **94** 049904 (erratum)
[12] Blencowe M P 2005 *Preprint* cond-mat/0502566
[13] Mozyrsky D and Martin I 2002 *Phys. Rev. Lett.* **89** 018301
[14] Smirnov A Y, Mourokh L G and Horing N J M 2003 *Phys. Rev.* B **67** 115312
[15] Lehnert K W 2005 unpublished work
[16] Averin D V and Aleshkin V Y 1989 *JETP Lett.* **50** 367
    Averin D V and Aleshkin V Y 1990 *Physica (Amsterdam)* **165–166B** 949
[17] van den Brink A M, Schon G and Geerligs L J 1991 *Phys. Rev. Lett.* **67** 3030
[18] Blencowe M P, Imbers J and Armour A D 2005 *New J. Phys.* **7** 236
[19] Braginsky V B and Manukin A B 1967 *Sov. Phys.—JETP* **25** 653
[20] Metzger C H and Karrai K 2004 *Nature* **432** 1002
[21] Harris J G E 2005 in preparation
[22] Clerk A A 2004 *Phys. Rev.* B **70** 245306
[23] Schoelkopf R J, Clerk A A, Girvin S M, Lehnert K W and Devoret M H 2003 *Quantum Noise in Mesoscopic Systems* ed Y Nazarov (Amsterdam: Kluwer) pp 175–203 (*Preprint* cond-mat/0210247)
[24] Korotkov A N 1994 *Phys. Rev.* B **49** 10381
[25] Averin D V 2000 *Preprint* cond-mat/0010052
[26] Johansson G, Kack A and Wendin G 2002 *Phys. Rev. Lett.* **88** 046802
[27] van den Brink A M 2002 *Europhys. Lett.* **58** 562
[28] Clerk A A, Girvin S M, Nguyen A K and Stone A D 2002 *Phys. Rev. Lett.* **89** 176804
[29] Tinkham M 1996 *Introduction to Superconductivity* (New York: McGraw-Hill)
[30] Dynes R C, Narayanamurti V and Garno J P 1978 *Phys. Rev. Lett.* **41** 1509
[31] Nakamura Y, Chen C D and Tsai J S 1996 *Phys. Rev.* B **53** 8234
[32] Choi M S, Plastina F and Fazio R 2001 *Phys. Rev. Lett.* **87** 116601
    Choi M S, Plastina F and Fazio R 2003 *Phys. Rev.* B **67** 045105
[33] Esteve D 1992 *Single Charge Tunneling* ed H Grabert and M H Devoret (New York: Plenum) pp 109–137
[34] Lehnert K W, Bladh K, Spietz L F, Gunnarsson D, Schuster D I, Delsing P and Schoelkopf R J 2003 *Phys. Rev. Lett.* **90** 027002
[35] Caves C M 1982 *Phys. Rev.* D **26** 1817–39
[36] Clerk A A 2003 *New Directions in Mesoscopic Physics* ed R Fazio, V F Gantmakher and Y Imry (Dordrecht: Kluwer) p 325 (*Preprint* cond-mat/0203338)
[37] Braginsky V B and Tikhonov A B M M Y 1970 *Sov. Phys.—JETP* **31** 829
[38] Braginsky V B and Manukin A B 1977 *Measurements of Weak Forces in Physics Experiments* (Chicago, IL: Chicago University Press)
[39] Marquardt F, Harris J G E and Girvin S M 2005 *Preprint* cond-mat/0502561
[40] Risken H 1996 *The Fokker–Planck Equation* (Berlin: Springer)
[41] Kramers H A 1941 *Physica* **7** 284